Aust. J. Phys., 1988, 41, 477–85

Measurement of Thermal Diffuse Scattering Using Pulsed Neutron Diffraction*

B. T. M. Willis

Chemical Crystallography Laboratory, University of Oxford,
9 Parks Rd, Oxford OX1 3PD, England.
Atomic Energy Research Establishment,
Harwell, Oxon OX11 0RA, England.

Abstract

Collective excitations in crystals can be examined with neutrons by means of the so-called 'diffraction method', without carrying out an energy analysis of the inelastically scattered neutrons. For studying thermal diffuse scattering (TDS) from acoustic phonons, it is particularly advantageous to employ a white source of pulsed neutrons instead of a monochromatic source of reactor neutrons. Provided that the neutron velocity is less than the sound velocity in the crystal, each reciprocal-lattice point observed in backscattering Laue geometry is associated with a wavelength window within which TDS is forbidden. The edges of the window are readily measured to give the sound velocity as a function of the direction of propagation.

1. Introduction

The so-called 'diffraction method' of studying collective excitations in crystals was first suggested by Elliott and Lowde (1955). A continuous source of neutrons of fixed wavelength is employed, and those neutrons which are scattered inelastically by the sample are observed without the necessity of performing an energy analysis. The method has been widely adopted for measuring magnetic spin waves in ferromagnetic and ferrimagnetic materials (Alperin *et al.* 1967 and references therein). It has been used rather less for the study of thermal excitations, or TDS.

In this paper it will be shown that, by replacing the continuous source from a nuclear reactor with a pulsed source, the examination of TDS by the diffraction method becomes especially attractive. First, the theory will be covered briefly (Sections 2 and 3) and then a few experimental results obtained with the pulsed neutron source ISIS at the Rutherford Appleton Laboratory will be described.

2. Scattering Surfaces for Elastic and Inelastic (One-phonon) Processes

In a neutron scattering experiment an incident neutron of wave vector $\boldsymbol{k}_0$ is converted into a scattered neutron of wave vector $\boldsymbol{k}$. The wavelengths of the incident and scattered radiation are $2\pi/k_0$ and $2\pi/k$ respectively, and the angle between them is the scattering angle 2θ. For an elastic process, such as Bragg scattering, there is no change of energy (or wavelength) on scattering:

$$k = k_0 . \tag{1}$$

* Paper presented at the International Symposium on Accuracy in Structure Factor Measurement, held at Warburton, Australia, 23–26 August 1987.

0004-9506/88/030477$03.00

For an inelastic process, there is an exchange of energy between the neutrons and the crystal, so that $k > k_0$ for energy gain (loss of energy by crystal), or $k < k_0$ for energy loss (gain of energy by crystal).

The 'scattering surface' is defined as the locus in reciprocal space of the endpoints of all wave vectors $\boldsymbol{k}$ undergoing a particular scattering process. We shall derive the topology of the scattering surfaces for both elastic scattering and for inelastic scattering in which the crystal exchanges one quantum of vibrational energy (phonon) with the incident radiation. These surfaces provide the key to understanding the nature of the TDS in a diffraction experiment. The surfaces are quite different for continuous (fixed wavelength) neutrons and for pulsed (white) neutrons.

(a) Elastic Scattering: Continuous Neutrons of Fixed Wavelength

In Fig. 1 we draw a reciprocal lattice with origin at O, and with an *hkl* point P whose distance from O is

$$\mathrm{OP} = 2\pi/d_{hkl}.$$

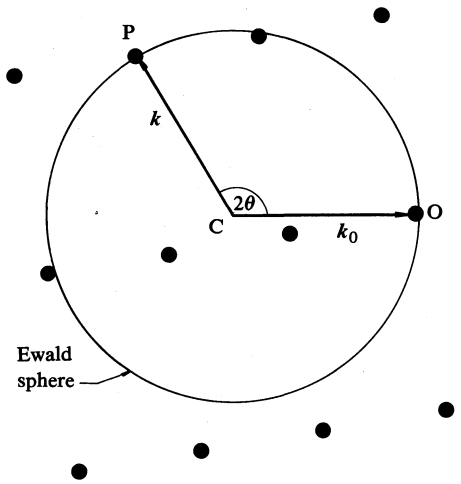

Fig. 1. Elastic scattering surface for fixed incident wavelength and variable scattering angle.

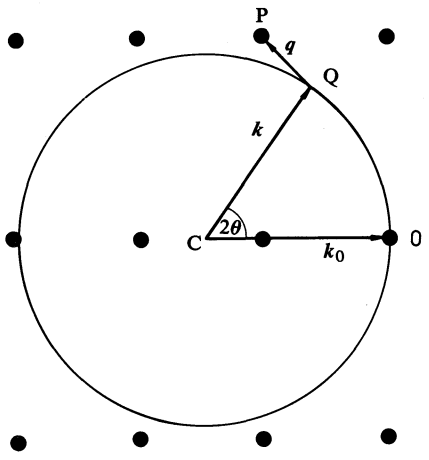

Fig. 2. Inelastic scattering surface for X-rays for fixed incident wavelength and variable scattering angle.

Then if CO represents the wave vector of the incident radiation, the locus of the tip of the scattered wave vector $\boldsymbol{k}$ is the Ewald sphere with centre C. This sphere is the scattering surface for *all* elastic processes, such as those associated with isotope or spin disorder. Bragg scattering is also an elastic process, but the interference conditions are satisfied only when the sphere passes directly through a reciprocal-lattice point (e.g. P in Fig. 1).

(b) Inelastic Scattering: Continuous Neutrons of Fixed Wavelength

If the sphere does not pass through P, no Bragg scattering occurs but inelastic scattering is possible (see Fig. 2). The condition for the conservation of momentum requires that the momentum $\hbar\boldsymbol{q}$ is exchanged between the radiation and the crystal: $\boldsymbol{q}$ is represented by the vector **PQ** and is the wave vector of the lattice vibration, or phonon, which participates in the scattering process.

Fig. 2 has been drawn on the assumption that $k_0 = k$, i.e. that the energy of a phonon is negligible compared with the energy of a quantum of the incident radiation. It applies, therefore, to X-ray scattering but not to neutron scattering, where the phonon energy is comparable with the energy of the neutron itself. The scattering surface for TDS of X-rays is the Ewald sphere, and the TDS intensity recorded in a fixed direction 2θ, defined by **CQ** in Fig. 2, is calculated by connecting Q to the closest point P of the reciprocal lattice. When 2θ changes, a different phonon $\boldsymbol{q}$ is selected but the intensity of the TDS always remains finite.

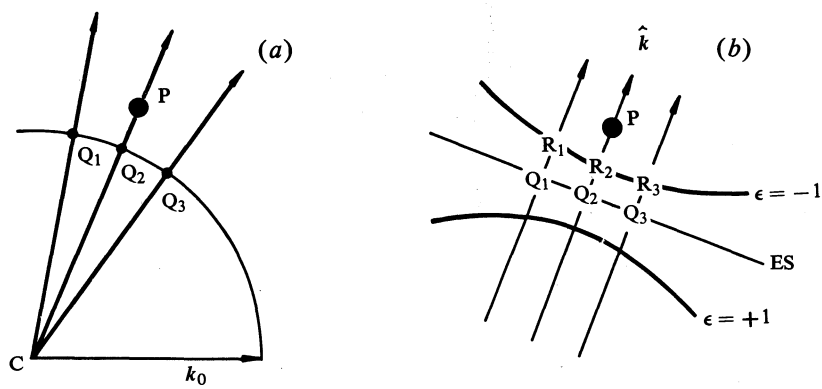

Fig. 3. (*a*) Elastic scattering surface close to the reciprocal-lattice point P. (*b*) Corresponding one-phonon inelastic scattering surfaces, where PR = q and RQ = $k - k_0$. Both diagrams apply to neutrons of fixed incident wavelength and variable scattering angle.

For neutrons which are scattered by vibrations of low frequency (acoustic modes of low q), conservation of energy requires that (Willis 1986)

$$k - k_0 = -\epsilon\beta q, \tag{2}$$

where ϵ is either $+1$ or -1; $+1$ refers to phonon emission (by the crystal) or neutron energy loss and -1 to phonon absorption or neutron energy gain. Further, β is the ratio c_s/v_n, where c_s is the sound velocity in the crystal and v_n is the neutron velocity. In Fig. 3*a* we draw the scattering diagram for neutrons scattered along

CQ_1, CQ_2, CQ_3 close to the reciprocal-lattice point P. The same diagram is shown enlarged and simplified in Fig. 3*b*: the Ewald sphere in (*a*) is replaced by its tangent plane in (*b*) and the scattered neutrons emerge in a parallel bundle. We readily see that equation (2) now demands that the inelastic scattering surface is a second-order conic. For any point R on the surface, the perpendicular distance from the plane ES is $k-k_0$ and the distance PR is the wave number q. If $\beta < 1$ the surface is a hyperboloid of two sheets (Fig. 3*b*), whereas for $\beta > 1$ it is an ellipsoid which has P at one focus (see Fig. 7*b*).

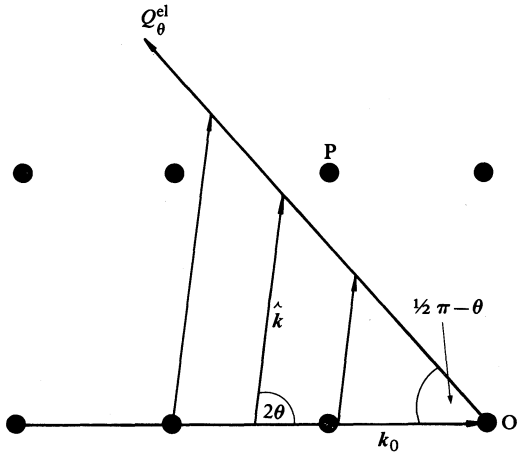

Fig. 4. Elastic scattering surface for 'white' incident beam and fixed scattering angle.

(c) Elastic Scattering: Pulsed Neutrons

In a pulsed neutron experiment we employ Laue diffraction geometry, in which there is a continuous range of wavelengths incident on a crystal of fixed orientation. Fig. 4 is the diagram for elastic scattering, where the angle between the scattered neutrons and the incident direction is set at 2θ.

The vector $\boldsymbol{Q}_\theta^{el}$, which lies in the scattering plane and is inclined at $\frac{1}{2}\pi-\theta$ to the incident beam, is the locus of the end points of $\boldsymbol{k}$ for all elastic scattering events. There is no Bragg scattering from the point P, unless the crystal orientation is altered to bring P into coincidence with $\boldsymbol{Q}_\theta^{el}$. The wavelength which is Bragg reflected is then

$$\lambda_B = 2\pi/k_0 = 4\pi \sin\theta/|\boldsymbol{B}_{hkl}|,$$

where $|\boldsymbol{B}_{hkl}|$ is the length of the vector **OP**, and there is no reflection of the remaining wavelengths.

In two dimensions the elastic scattering surface is a straight line, $\boldsymbol{Q}_\theta^{el}$, through the origin. In three dimensions the locus is a right-circular cone with its axis along the incident direction and with semi-angle $\frac{1}{2}\pi-\theta$.

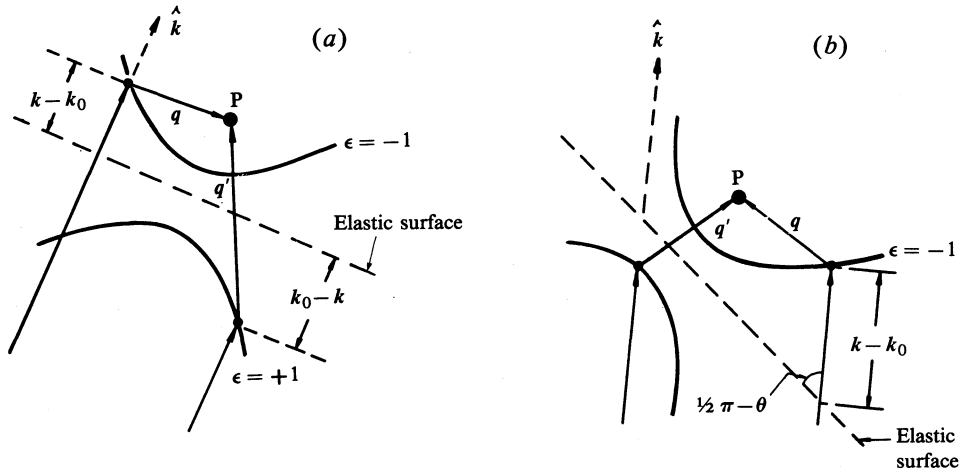

Fig. 5. Inelastic scattering surface for (*a*) continuous (reactor) neutrons with fixed k_0 and $e = \beta^{-1}$ and (*b*) pulsed neutrons with variable k_0 and $e = (\beta \cos\theta)^{-1}$.

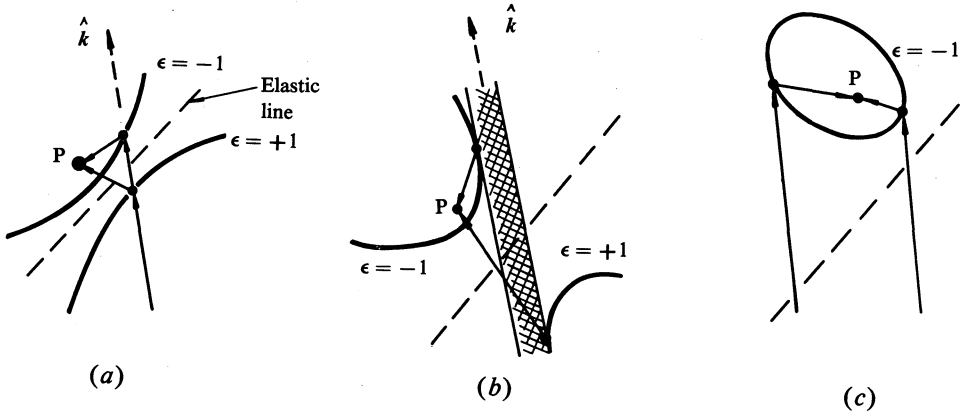

Fig. 6. Inelastic scattering surfaces for pulsed neutrons and for three ranges: (*a*) $\beta < 1$; (*b*) $1 < \beta < \sec\theta$; and (*c*) $\beta > \sec\theta$. In (*b*) no TDS can occur in the shaded region.

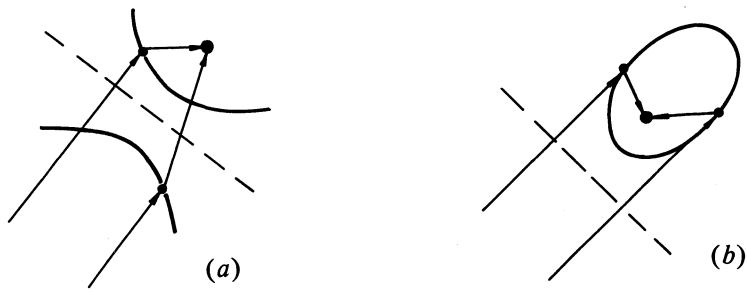

Fig. 7. Inelastic scattering surfaces for reactor neutrons and for two ranges: (*a*) $\beta < 1$ and (*b*) $\beta > 1$.

(d) Inelastic Scattering: Pulsed Neutrons

Equation (2) again expresses the condition determining the nature of the scattering surface for inelastic scattering. However, there is a crucial difference in the geometrical interpretation of equation (2), for the case of reactor neutrons (Fig. 5*a*) and of pulsed neutrons (Fig. 5*b*). This difference arises because the scattered radiation is normal to the elastic scattering surface in (*a*) but is inclined to it at an angle $\frac{1}{2}\pi-\theta$ in (*b*).

The distance of any point on the scattering surface from the fixed point P is q, and the distance of the same point from the elastic line is $-\epsilon(k-k_0)\cos\theta$. From equation (2) the ratio of these distances is $e = (\beta\cos\theta)^{-1}$, so that the one-phonon scattering surface is a conic of eccentricity e. (We assume that β is constant, i.e. that the sound waves propagate in all directions with the same velocity.) The eccentricity, therefore, is β^{-1} for a fixed-wavelength experiment, but $(\beta\cos\theta)^{-1}$ for a Laue experiment.

Now it is readily shown (Willis 1986; Schofield and Willis 1987) that, provided the neutron velocity exceeds the sound velocity ($\beta < 1$), one-phonon scattering occurs for both energy loss ($\epsilon = +1$) and energy gain ($\epsilon = -1$). On the other hand if $\beta > 1$, scattering takes place either by energy loss or by energy gain, but not by both processes. We also have the condition that $\beta\cos\theta < 1$ for the scattering surface to be represented by a hyberboloid of two sheets, and the condition $\beta\cos\theta > 1$ for the surface to be an ellipsoid of revolution. Hence, there are three characteristic ranges of β: (*a*) $\beta < 1$; (*b*) $1 < \beta < \sec\theta$; and (*c*) $\beta > \sec\theta$. These are illustrated in Fig. 6. If $\theta \to 0$, range (*b*) contracts to nothing, and we have just two ranges, $\beta < 1$ and $\beta > 1$, as for the case of reactor neutrons (Fig. 7). On the other hand, if $\theta \to \frac{1}{2}\pi$, range (*c*) contracts to nothing and the ranges (*a*) and (*b*) remain.

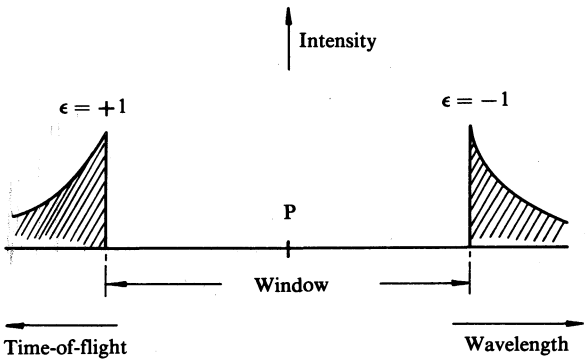

Fig. 8. TDS intensity against incident wavelength when β lies in the range $1 < \beta < \sec\theta$ (schematic).

3. The Wavelength Window

Range (*b*) with β between 1 and $\sec\theta$ has no counterpart in fixed-wavelength geometry. This range is of especial importance for pulsed neutron diffraction, because of the existence of a 'wavelength window' in the incident white beam, which encompasses the Bragg wavelength and for which TDS is forbidden. In Fig. 8 we show schematically the variation with incident wavelength of the intensity of the TDS

in the neighbourhood of the reciprocal-lattice point, when the ratio c_s/v_n lies in the range $1 < \beta < \sec\theta$ and when the crystal is off-set by $\Delta\theta$ $(=\theta-\theta_B)$ from the Bragg setting.

Clearly, the possibility of observing the wavelength window increases with increasing scattering angle 2θ. In the backscattering instrument High Resolution Powder Diffractometer (HRPD) at ISIS (Johnson and David 1985) 2θ is very close to 180° and $\sec\theta$ is as high as 50. This means that, for such an instrument, we can ignore range (*c*) (with $\beta > \sec\theta$) and consider that the TDS occurs either in range (*a*), $\beta < 1$, without a wavelength window, or in range (*b*), $\beta > 1$, with a window.

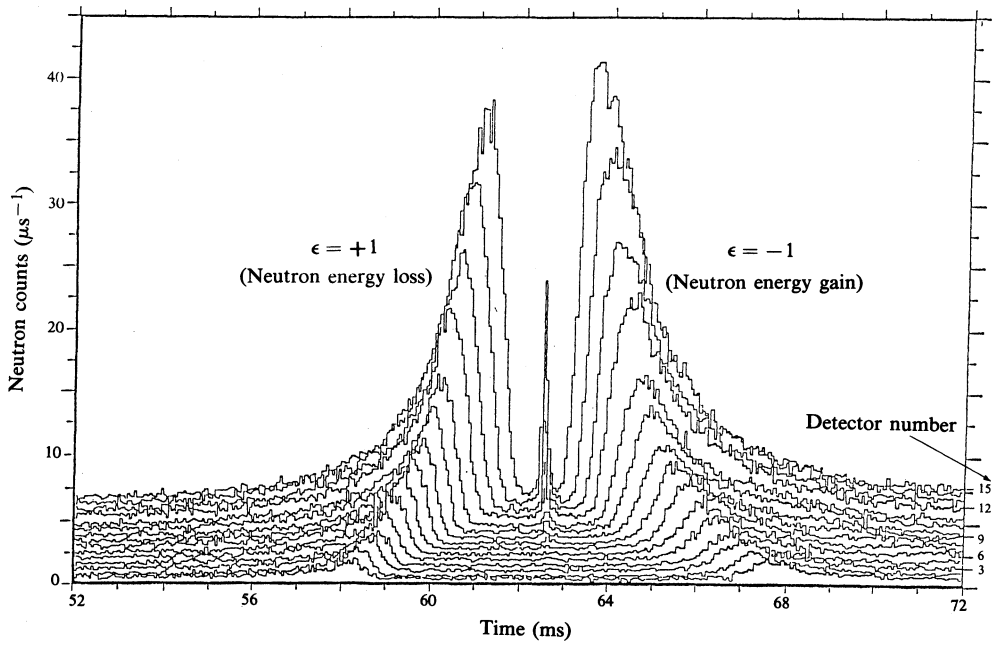

Fig. 9. Pattern of TDS around the (422) Bragg reflection with $\theta_B = 85{\cdot}1°$ from barium fluoride, showing the variation of intensity with time-of-flight (wavelength) and with off-set $\Delta\theta$ from the Bragg angle. The intensity was recorded in fifteen detectors: detector 15, $\Delta\theta = 1{\cdot}1°$; detector 14, $\Delta\theta = 1{\cdot}3°$; detector 13, $\Delta\theta = 1{\cdot}5°$, etc.; and detector 1, $\Delta\theta = 3{\cdot}9°$.

The TDS at the edges of the window rises to an abrupt maximum, as shown in Fig. 9 for barium fluoride. The wavelength separation $\Delta\lambda$ between the two edges of the window is given by (Willis 1986):

$$\Delta\lambda/\lambda_B = 2(\beta^2-1)^{\frac{1}{2}}\Delta\theta, \tag{3}$$

where it is assumed that $\theta = 90°$. Hence the width of the window increases steadily with the off-set angle (see Fig. 9) and a plot of $\Delta\lambda/\lambda_B$ versus $\Delta\theta$ yields the velocity ratio β. Using Fig. 9 this plot gives $\beta = 1{\cdot}455$. However, $v_n = h/2m_n d_{hkl} = 1{\cdot}571\ \mathrm{km\,s^{-1}}$ for the 422 reflection and so we have $c_s = 2{\cdot}286\ \mathrm{km\,s^{-1}}$. This compares with the value $c_s = 2{\cdot}275\ \mathrm{km\,s^{-1}}$ for the transverse acoustic velocity, as deduced from measurements of the elastic constants.

Barium fluoride is acoustically isotropic, and so β is a constant for a given reciprocal-lattice point. In equation (3) and in the theory outlined in Section 2 isotropic behaviour has been assumed. But an isotropic crystal is rarely found, even in the cubic system, and so in general β is dependent on the direction of propagation of the acoustic wave.

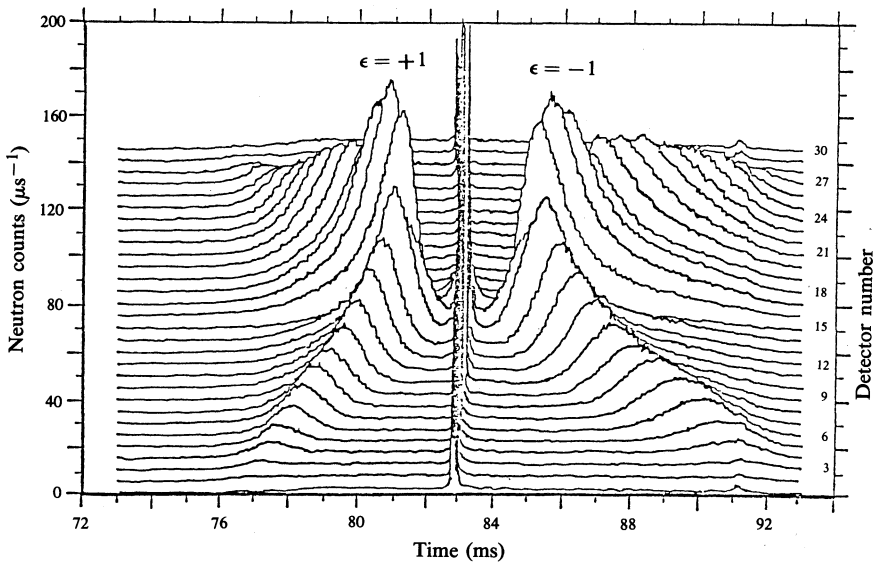

Fig. 10. Pattern of TDS around the (004) Bragg reflection with $\theta_B = 90{\cdot}0°$ from pyrolytic graphite. The intensity was recorded in thirty detectors, 1 to 30. For detectors 1 to 15 the neutrons were scattered to one side of the main beam, and for detectors 16 to 30 to the other side: detectors 15 and 16, $\Delta\theta = 1°$; detectors 14 and 17, $\Delta\theta = 1{\cdot}2°$; detectors 13 and 18, $\Delta\theta = 1{\cdot}4°$, etc.; and detectors 1 and 30, $\Delta\theta = 3{\cdot}8°$.

If ζ is the angle between the phonon wave vector $\boldsymbol{q}$ and the reciprocal-lattice vector **OP**, then

$$\zeta = \tfrac{1}{2}\pi + \epsilon \arcsin(1/\beta), \tag{4}$$

and so $\beta(\zeta)$ can be obtained by combining equations (3) and (4). [A full treatment of the anisotropic case is given by Schofield and Willis (1987), who showed that a principal modification in the theory is the replacement of the phase velocity in the definition of β by the group velocity.] The elastic properties of pyrolytic graphite are extremely anisotropic, and yet the TDS shown in Fig. 10 has been successfully analysed to give the sound velocity as a function of direction (Willis *et al.* 1986).

Acknowledgments

Work described in this paper was undertaken as part of the Underlying Research Programme of the UKAEA. The author is grateful to Dr C. J. Carlile and Dr W. I. F. David, both of the Rutherford Appleton Laboratory of the UK, for their help in the experimental measurements using the pulsed neutron source ISIS.

References

Alperin, H. A., Steinsvoll, O., Nathans, R., and Shirane, G. (1967). *Phys. Rev.* **154**, 508–14.
Elliott, R. J., and Lowde, R. D. (1955). *Proc. R. Soc. London* A **230**, 46–73.
Johnson, M. W., and David, W. I. F. (1985). Rutherford Appleton Laboratory Report RAL-85-112.
Schofield, P., and Willis, B. T. M. (1987). *Acta Cryst.* A **43**, 803–9.
Willis, B. T. M. (1986). *Acta Cryst.* A **42**, 514–25.
Willis, B. T. M., Carlile, C. J., Ward, R. C., David, W. I. F., and Johnson, M. W. (1986). *Europhys. Lett.* **2**, 767–74.

Manuscript received 25 August, accepted 4 December 1987